Inorganic Chemistry

Article

pubs.acs.org/IC

Switching a 2D Co(II) Layer to a 3D Co_7-Cluster-Based Metal–Organic Framework: Syntheses, Crystal Structures, and Magnetic Properties

Di-Ming Chen,[†] Xiao-Zhou Ma,[†] Xue-Jing Zhang, Na Xu,* and Peng Cheng*

Department of Chemistry, Key Laboratory of Advanced Energy Materials Chemistry (MOE), and Collaborative Innovation Center of Chemical Science and Engineering (Tianjin), Nankai University, Tianjin 300071, People's Republic of China

Supporting Information

ABSTRACT: Two 2D layered coordination networks with formulas of $\{[Co(TPA)Cl](H_2O)_{2.5}\}_n$ (**1**) and $\{[Co(TPA)(\mu_2\text{-}OH)](H_2O)_2\}_n$ (**2**) (HTPA = 4-(1,2,4-triazol-4-yl)-phenylacetic acid) were solvothermally synthesized and fully characterized. Interesting 1D Co^{2+}-Cl or Co^{2+}-μ_2-OH chain structures were observed. By carefully adjusting the reaction conditions, a new 3D metal–organic framework (MOF) with a formula of $\{[Co_7(TPA)_6(\mu_3\text{-}OH)_4(\mu_2\text{-}OH)_2(H_2O)_4](TPA)_2(DMF)_3(H_2O)_3\}_n$ (**3**) was obtained. MOF **3** is built from Co_7 clusters and fully deprotonated TPA ligands, which display a cubic pcu topology. Factors that influence the structures of the three TPA-based complexes, as well as their magnetic properties, were investigated in detail. The heptanuclear-Co(II)-cluster-based MOF **3** shows interesting magnetization dynamics at low temperature.

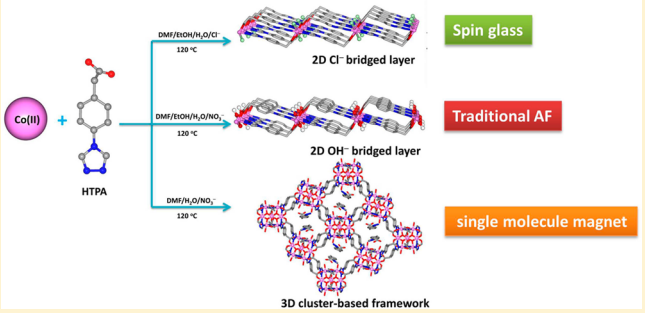

INTRODUCTION

The past decade has witnessed a rapid development in the design and construction of metal–organic frameworks (MOFs) for their intriguing structural features and potentially useful applications such as gas storage/separation,[1−5] catalysis,[6] sensors,[7,8] and molecular magnets.[9−13] MOFs with cluster-based SBU (secondary building blocks) have drawn particular attention for their interesting properties such as slow relaxation of the magnetization.[14−19] However, it is still a great challenge to obtain cluster-based MOFs rationally because the reaction processes are usually affected by many outside factors, including the coordination geometry of the metal ions, coordination models and abilities of the ligand, solvents, metal to ligand ratio, counterions, and so on.[20] Hence the selection of proper ligands is crucially important for this point. From a magnetic perspective, carboxylate ligands have shown great potentials in constructing molecular magnets (especially the Co(II)-carboxylate MOFs) exhibiting interesting magnetic behaviors, such as antiferromagnetism, ferrimagnetism, and spin canting.[21−27] Organic ligands containing heterocyclic triazolyl groups are another type of bridging ligands for cluster-based MOFs to show spin frustration, antiferromagnetism, long-range magnetic ordering, meta-magnetism, and spin canting.[28−34] So the combination of both carboxylate-triazole groups and metal clusters into MOFs may result in diversiform structures and interesting properties.[35,36] Recently, we have successfully constructed a cage-based cationic MOF by using a bifunctional linker, 4-(4-carboxyphenyl)-1,2,4-triazole (HCPT), and a $[Cu_4Cl]^{7+}$ cluster as the node.[37] As a continuation of our work, another bifunctional organic linker, 4-(1,2,4-triazol-4-yl)phenylacetic acid (HTPA), was designed and synthesized (Scheme 1). Solvothermal reaction of HTPA with different Co(II) salts under similar conditions afforded two isometric 2D bilayer networks, namely, $\{[Co(TPA)Cl](H_2O)_{2.5}\}_n$ (**1**) and $\{[Co(TPA)(\mu_2\text{-}OH)](H_2O)_2\}_n$ (**2**), assembled by interesting 1D Co^{2+}-Cl or Co^{2+}-μ_2-OH chains. Through carefully adjusting the reaction conditions, a novel heptanuclear $\{Co_7(OH)_6\}$ cluster-based MOF, $\{[Co_7(TPA)_6(\mu_3\text{-}OH)_4(\mu_2\text{-}OH)_2(H_2O)_4]$-

Scheme 1. Synthetic Routes for Complexes 1−3

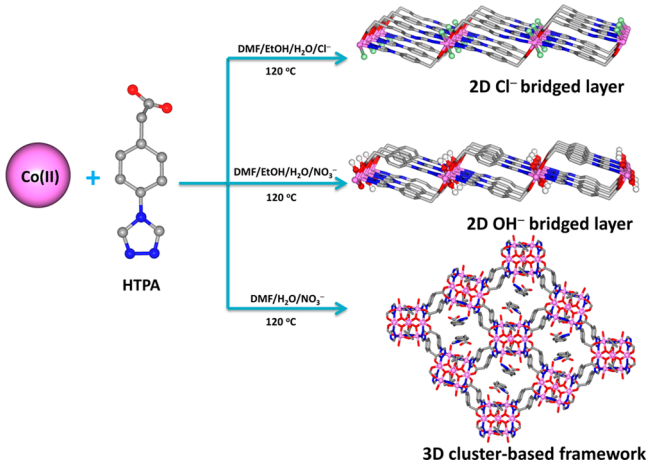

Received: January 9, 2015
Published: March 2, 2015

DOI: 10.1021/acs.inorgchem.5b00074
Inorg. Chem. 2015, 54, 2976−2982

Table 1. Crystallographic Data and Structure Refinement Details of 1−3

	1	2	3
empirical formula	$C_{10}H_{13}ClCoN_3O_{4.5}$	$C_{10}H_{13}CoN_3O_5$	$C_{89}H_{105}Co_7N_{27}O_{32}$
fw	341.61	314.16	2477.48
temp (K)	129(2)	129(2)	129(2)
cryst syst	monoclinic	monoclinic	monoclinic
space group	C_2/m	$P2_1/c$	$P2_1/n$
a (Å)	17.687(2)	11.4105(9)	14.4430(7)
b (Å)	7.2468(7)	6.9570(3)	22.1987(13)
c, (Å)	11.5369(10)	15.5927(9)	17.7628(12)
α (deg)	90.00	90.00	90.00
β (deg)	108.467(11)	95.977(6)	103.975(6)
γ (deg)	90.00	90.00	90.00
V (Å^3)	1402.6(2)	1231.1(1)	5526.5(6)
Z	2	4	2
D_c (g/cm^3)	1.632	1.695	1.325
μ (mm^{-1})	1.434	1.415	1.098
R_{int}	0.0633	0.0582	0.0392
no. of reflns collected/unique	2631/1344	4262/2172	28 118/9718
GOF on F^2	1.044	1.052	1.080
R_1, wR_2 $[I > 2\sigma(I)]$	0.0641, 0.1531	0.0545, 0.1308	0.0587, 0.1728
R_1, wR_2 (all data)	0.0929, 0.1715	0.0723, 0.1498	0.0717, 0.1818
largest peak, hole (e Å^{-3})	1.16/−0.74	0.84/−0.85	2.67/−0.68

$(TPA)_2(DMF)_3(H_2O)_3\}_n$ (**3**), was obtained, which is first observed as an SBU in MOF chemistry. Moreover, their magnetic properties were also studied and discussed in detail.

EXPERIMENTAL SECTION

Materials and Methods. HTPA was synthesized according to the reported literature.[38] Other reagents are commercially available and were used without further purification. Elemental analyses (EA) for C, H, and N were performed on a PerkinElmer analyzer. FT-IR spectra were measured on a Bruker Tensor 27 spectrometer on KBr discs in the range 4000−400 cm^{-1}. Thermogravimetric analyses (TGA) were carried out in a Labsys NETZSCH TG 209 Setaram apparatus from room temperature to 800 °C under a N_2 atmosphere with a heating rate of 10 °C min^{-1}. Powder X-ray diffraction (PXRD) patterns were recorded on a D/Max-2500 X-ray diffractometer with Cu Kα radiation. Magnetic measurements were performed on a Quantum Design SQUID VSM magnetometer. Diamagnetic corrections were made with both Pascal's constants and a sample holder.

Synthesis of $\{[Co(TPA)Cl](H_2O)_{2.5}\}_n$ (1). A mixture of $CoCl_2\cdot 6H_2O$ (0.048 g, 0.2 mmol) and HTPA (0.020 g, 0.1 mmol) was added to a mixed solvent of DMF (2 mL), EtOH (4 mL), and H_2O (1 mL) and then heated at 120 °C for 72 h in a 23 mL Teflon bomb. Red needle-like crystals were obtained after cooling to room temperature. The yield was 60% (based on HTPA). IR (cm^{-1}): 3416 (br), 3065 (w), 1676 (s), 1589 (s), 1388 (s), 1245 (w), 1184 (w), 1095 (m), 835 (m), 789 (m), 746 (s), 708 (s), 639 (w), 485 (m). Anal. Calcd (%) for **1** ($C_{10}H_{13}ClCoN_3O_{4.5}$): C 35.16, H 3.84, N 12.30. Found: C 35.02, H 3.52, N 12.41.

Synthesis of $\{[Co(TPA)(\mu_2\text{-}OH)](H_2O)_2\}_n$ (2). A mixture of $Co(NO_3)_2\cdot 6H_2O$ (0.045 g, 0.15 mmol), HTPA (0.020 g, 0.1 mmol), DMF (2 mL), EtOH (4 mL), and H_2O (4 mL) was added to a 23 mL Teflon bomb and then heated at 120 °C for 3 days. Red, needle-like crystals were obtained after cooling the reaction mixture to room temperature. The yield was 75% (based on HTPA). IR (cm^{-1}): 3458 (br), 3045 (br), 1605 (s), 1385 (s), 1219 (w), 1070 (m), 1346 (m), 1306 (w), 1107 (s), 1007 (w), 914 (w), 831 (w), 741 (w), 619 (s). Anal. Calcd (%) for **2** ($C_{10}H_{13}CoN_3O_5$): C 38.23, H 4.17, N 13.38. Found: C 38.19, H 4.25, N 13.24.

Synthesis of $\{[Co_7(TPA)_6(\mu_3\text{-}OH)4(\mu_2\text{-}OH)_2(H_2O)_4](TPA)_2(DMF)_3(H_2O)_3\}_n$ (3). A mixture of $Co(NO_3)_2\cdot 6H_2O$ (0.060 g, 0.2 mmol), HTPA (0.040 g, 0.2 mmol), DMF (2.5 mL), and H_2O (2.5 mL) was added to a 23 mL Teflon bomb, and then heated to 120 °C for 36 h. After cooling to room temperature during a period of 60 h, yellowish block crystals suitable for single-crystal X-ray study were harvested. The yield was 53% (based on HTPA). IR (cm^{-1}): 3422 (br), 3018 (br), 1594 (s), 1384(s), 1107 (s), 1016 (s), 867 (m), 815 (s), 790 (m), 747 (m), 707 (m), 620 (m). Anal. Calcd (%) for **3** ($C_{89}H_{105}Co_7N_{27}O_{32}$): C, 43.15; H, 4.27; N, 15.26. Found: C 43.59, H 4.38, N 15.08.

X-ray Crystallography. Crystallographic data for **1**−**3** were collected at 129 K on an Oxford Supernova diffractometer with Mo Kα radiation (λ = 0.710 73 Å) using the ω-scan technique. The structures were solved by direct methods and refined with the full matrix least-squares technique with SHELXL-97 programs.[39] The highly disordered guest molecules of **3** are difficult to model, so their contribution of densities was modeled using the SQUEEZE routine in PLATON.[40] Final chemical formula of **3** was obtained from crystallographic data with EA and TGA data. Crystal data of **1**−**3** are summarized in Table 1.

RESULTS AND DISCUSSION

Synthesis and Structures. Complexes **1**−**3** were obtained under different synthetic conditions. Specifically, for **1** and **2**, a solvent mixture of DMF, EtOH, and water was used in the crystallization process. A clear solution was obtained in a DMF/H_2O (1:1) solvent mixture. A large number of insoluble solids was found when a DMF/EtOH (1:1) solvent mixture was used. After many tries, we found that a solvent mixture of DMF, EtOH, and water can give pure crystals of **1** and **2**. The bridged counteranion in the 1D Co(II) chains of **1** and **2** can be altered by using different Co(II) salts: when $CoCl_2$ was used as the starting material, a Cl^- bridge was found in **1**, and a μ_2-OH bridge was found in **2** by using $Co(NO_3)_2$ as the starting material. It has been noted that the ratio of Co(II) salts to HTPA ligand played a significant role in the yields and purity of the resulting products, and the best Co^{2+}/HTPA ratios are 2:1 for complex **1** and 1.5:1 for complex **2**, respectively. Cluster-based MOF **3** was obtained through subtle modification of reaction conditions by increasing the concentration of starting materials, while the reaction took place at the same temperature as that of **1** and **2**. The crystallization of **3** was optimized by varying the ratio of $Co(NO_3)_2$ and HTPA and a gradual cooling

DOI: 10.1021/acs.inorgchem.5b00074
Inorg. Chem. 2015, 54, 2976−2982

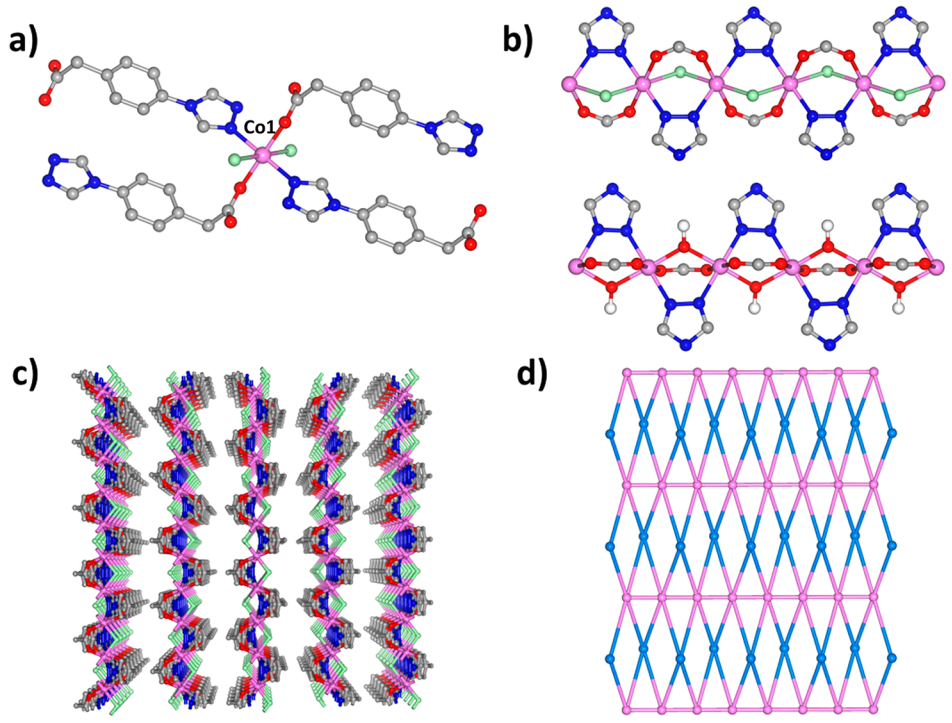

Figure 1. (a) Coordination environment of the Co(II) ion in **1** (all solvent molecules and H atoms were deleted for clarity). (b) Cl^- and OH^- bridged 1D Co(II) chains for **1** and **2**. (c) ABAB packing mode of the 2D layer for **1**. (d) Simplified 2D layer for **1** and **2**.

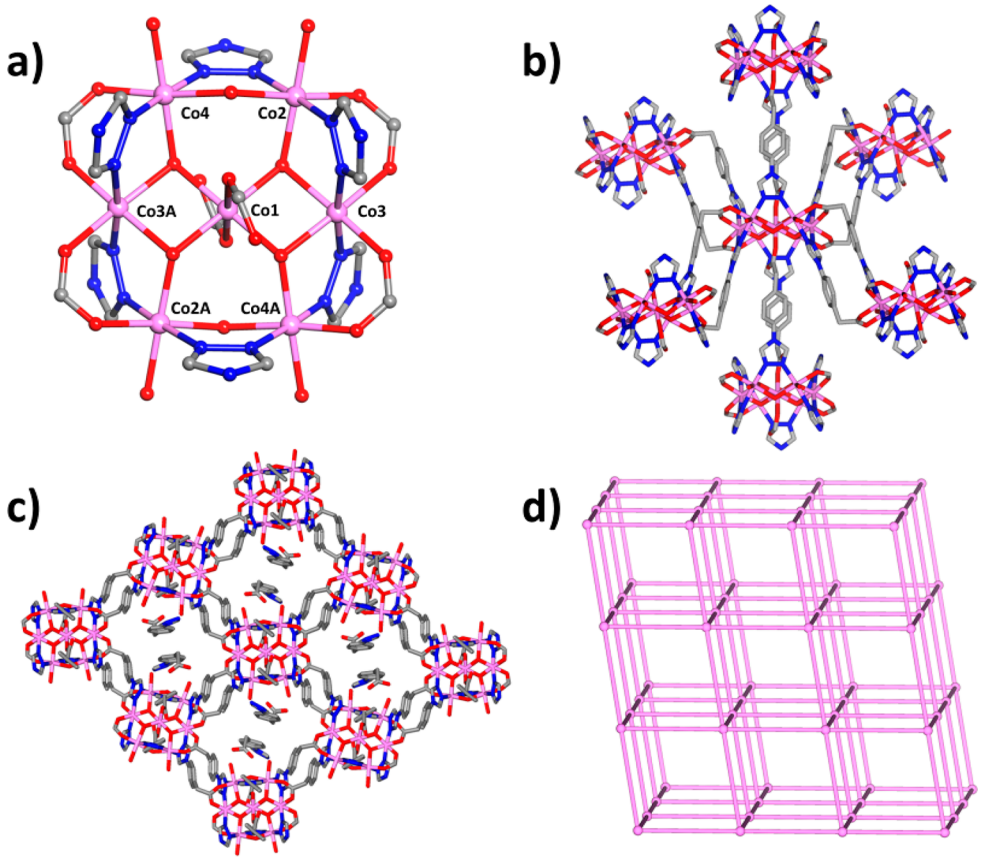

Figure 2. (a) Heptanuclear Co(II) cluster observed in **3** (symmetry code A: 1−*x*, −*y*, 1−*z*, all solvent molecules and H atoms were deleted for clarity). (b) View of the 6-connected heptanuclear Co(II) clusters via double-walled mode. (c) 3D framework of **3**. (d) Topological representation of the 6-connected pcu network.

DOI: 10.1021/acs.inorgchem.5b00074
Inorg. Chem. 2015, 54, 2976−2982

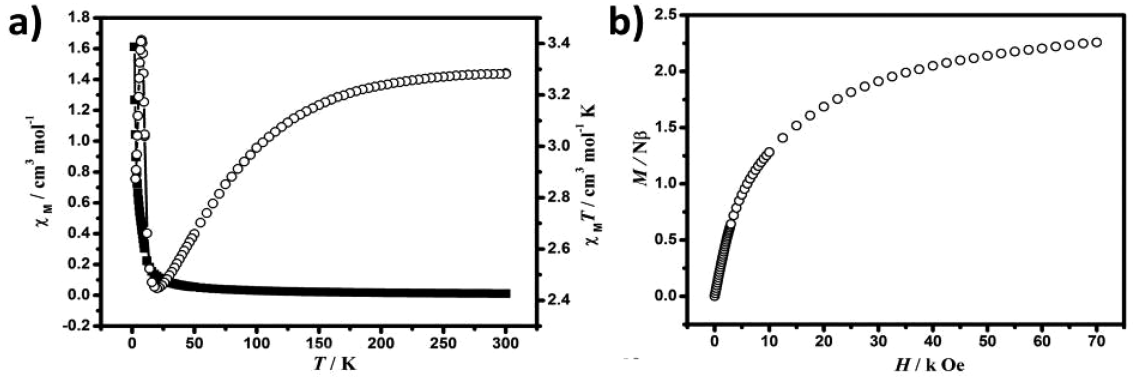

Figure 3. (a) Temperature dependence of $\chi_M T$ for **1**. (b) Field dependence of magnetization for **1**.

procedure for the isolation of X-ray quality single crystals. Especially, the quality of **3** was dependent upon the amount of HTPA in the solvent mixture, which may be due to the template effect of HTPA in the crystallization of **3**. This hypothesis is further evidenced by the free TPA^- ligands housed in the channels resolved by single-crystal X-ray diffraction.

Crystal Structures of 1 and 2. Although **1** and **2** crystallize in different space groups, they possess quite similar structures; thus only the structure of **1** was discussed in detail. **1** crystallizes in the monoclinic space group C_2/m and consists of a 2D bilayered structure. The asymmetric unit of **1** contains half of a crystallographically independent Co(II) ion, half of a TPA^- ligand, half of a Cl^- ion, and one and a quarter water molecules. The six-coordinated Co(II) ion connects with two oxygen atoms and two nitrogen atoms from four individual TPA^- ligands and is further bridged by two Cl^- ions, resulting in a distorted $[CoO_2N_2Cl_2]$ octahedral coordination geometry (Figure 1a). The Co−O bond distance is 2.062(3) Å, and the Co−N bond distance is 2.108(4) Å. Two adjacent Co(II) ions are linked together by one triazolate group, one carboxylate group, and one bridged Cl^- ion with a distance of 3.623(4) Å to give a 1D chain (Figure 1b). The completely deprotonated TPA^- ligand connects the adjacent chains to afford a 2D bilayered structure with square channels (Figure 1c). Taking the Co(II) ion as a six-connected node and the ligand as a four-connected node, the 2D network can be simplified as a 2-nodal (4,6)-connected topology with the point symbol $\{3^2.4^2.5^2\}\{3^4.4^4.5^4.6^3\}$ (Figure 1d).[41] **2** crystallizes in the monoclinic $P2_1/c$ space group, the Co−O bond distances are in the range 2.039(3) to 2.088(3) Å, and the Co−N bond distance is 2.125(4) Å. Two adjacent Co(II) ions are linked together by one triazolate group, one carboxylate group, and one μ_2-OH with a distance of 3.479(4) Å. **2** possesses the same topology as **1**.

Crystal Structure of 3. MOF **3** possesses an unprecedented 6-connected 3D network based on heptanuclear Co(II) clusters (Figure 2a). The asymmetric unit of **3** contains three and a half independent Co(II) ions, three coordinated TPA^- ligands, two μ_3-OH, one μ_2-OH, and one lattice-free TPA^- ligand. All cobalt atoms are assigned as Co^{2+} ions, and μ_3-O and μ_2-O atoms as OH^- atoms as revealed by the BVS (bond valence sums) calculated results and charge balance.[42] All the Co(II) ions are six-coordinate but with three different coordination environments: Co1, locating on an inversion center, shows an octahedral sphere coordinated by six oxygen atoms from four μ_3-OH and two TPA^- ligands; Co2 shows an octahedron connected with four oxygen atoms from one μ_3-OH, one μ_2-OH, one coordinated water, one TPA^-, and two nitrogen atoms from two individual TPA^-; Co3 is octahedrally coordinated by four oxygen atoms, from two μ_3-OH and two TPA^-, and two nitrogen atoms from two TPA^-; Co4 adopts the same coordination mode as Co2. The lengths of Co−O bonds range from 2.007(1) to 2.171(4) Å, and the Co−N bond distances vary from 2.099(2) to 2.146(9) Å. Three symmetry-related Co2−Co2A, Co3−Co3A, and Co4−Co4A pairs (A: $1-x, -y, 1-z$) associated with Co1 are ligated by four μ_3-OH and two μ_2-OH to give a $[Co_7(\mu_3\text{-}OH)_4(\mu_2\text{-}OH)_2(COO)_8]^{2+}$ cluster with the nearest Co···Co distance of ca. 3.07 Å, which can also be viewed as two $[Co_3(\mu_3\text{-}OH)_2(\mu_2\text{-}OH)]^{3+}$ triangles sharing a Co1 vertex (Figure S1). Each Co_7 cluster is bonded with six adjacent Co_7 clusters via 12 TPA^- ligands in a double-walled model (Figure 2b). It is interesting to notice that the free lattice TPA^- ligands in the channels act as the counteranions to balance the charge of the framework (Figure 2c), which is consistent with the observation in the synthesis of **3**, indicating its template effect in crystallization. To simplify the structure of **3**, the heptanuclear Co(II) clusters and the ligands can be viewed as 6-connected and 2-connected nodes, respectively. The 3D structure can be viewed as a 6-connected pcu framework with the point symbol $\{4^{12}.6^3\}$ (Figure 2d). As we well know, **3** is the first example possessing a disc-like Co_7 unit in 3D MOFs.[43−47]

Powder X-ray Diffraction and Thermogravimetric Analyses. PXRD was carried out at room temperature to confirm the phase purity of **1**−**3** (Figure S3). The patterns of the as-synthesized materials very well match the simulated curves from the single-crystal structure data, suggesting their pure phases. The thermal stabilities of **1**−**3** have been determined by TGA in a N_2 atmosphere in the temperature range 25−800 °C (Figure S4). **1** shows a weight loss of 15.6% from 25 to 115 °C, corresponding to the loss of two and a half lattice H_2O molecules (calcd 15.1%). A sharp weight loss appeared from 358 °C, indicative of a collapse of the framework. For **2**, a weight loss of 11.8% in the range 25−171 °C occurred, corresponding to the loss of two lattice water molecules (calcd 13.2%), and the framework decomposed starting from 264 °C. For **3**, a weight loss of 16.1% appeared in the range 25−167 °C due to the release of four coordinated water, three DMF, and three free H_2O molecules (calcd 16%). The framework could be stable up to 243 °C, and further heating led to the decomposition of the framework.

Magnetic Properties. The similar structure of **1** and **2** along with the unique structural features of **3** inspired us to

DOI: 10.1021/acs.inorgchem.5b00074
Inorg. Chem. 2015, 54, 2976−2982

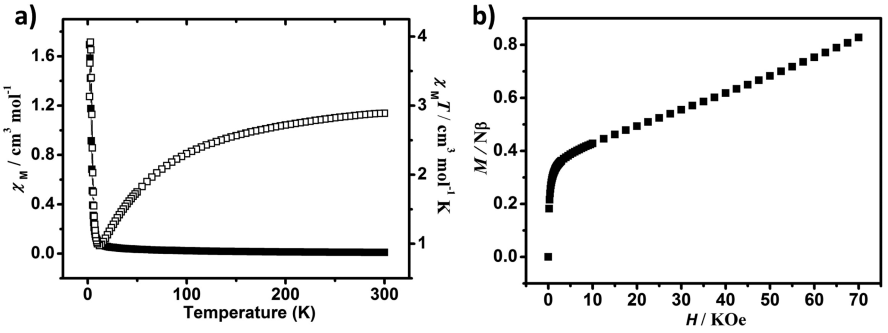

Figure 4. (a) Temperature dependence of χ_M and $\chi_M T$ of **2**. (b) Field dependence of magnetization for **2**.

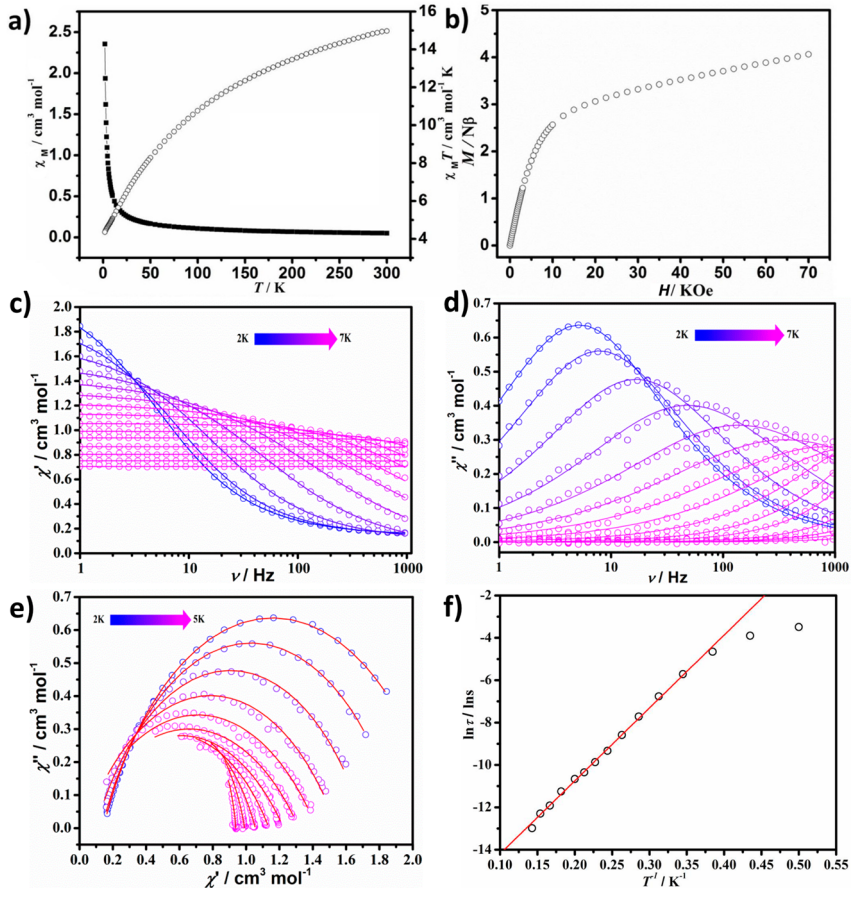

Figure 5. (a) Temperature dependence of χ_M and $\chi_M T$ of **3**. (b) Field dependence of magnetization for **3**. (c) In-phase (χ') ac susceptibility for **3** under 1800 Oe dc field. (d) Out-of-phase (χ'') ac susceptibility for **3** under 1800 Oe dc field. (e) Cole−Cole plots of **3** (the solid lines represent the best fits). (f) ln(τ) vs $1/T$ of **3**.

investigate the magnetic behaviors of the three complexes. The direct-current (dc) magnetic susceptibility of **1** was measured at 2−300 K at a dc field of 1000 Oe (Figure 3a). The $\chi_M T$ value of **1** at 300 K is 3.28 cm^3 mol^{-1} K, which is higher than the value (1.875 cm^3 mol^{-1} K) expected for one spin-only Co(II) ion (1.875 cm^3 mol^{-1} K, S = 3/2, g = 2) because of the strong spin−orbit coupling.[48−50] Upon lowering the temperature, the $\chi_M T$ first decreases to 2.46 cm^3 mol^{-1} K at 24 K, which is caused by spin−orbit coupling or antiferromagnetic interactions. Upon further lowering the temperature, the $\chi_M T$ increases suddenly to a maximum of 3.41 cm^3 mol^{-1} K at 7.58 K. The increase of $\chi_M T$ at 7−18 K might be attributed to the canted magnetic structure of the Co^{2+} chain.[51] The second decrease of $\chi_M T$ is due to the interchain antiferromagnetic interactions.[52] The fitting results of the $\chi_M T$ by the Fisher 1D model from 80 to 300 K reveal that J = −8.30 cm^{-1} and g = 2.71 (Figure S5a).[53−55] The negative J reveals interchain antiferromagnetic interactions between Co(II) ions. Due to the anisotropy of Co(II) in **1**, the M vs H curve displays that the magnetization increases to 2.26 Nβ without achieving saturation at 7 kOe (Figure 3b). Further analysis of the alternating-current (ac) susceptibility of **1** displays that the in-phase (χ') and out-of-phase (χ'') susceptibilities under zero dc fields show peaks at low temperature (Figure S6a). The frequency shift parameter φ of **1** is 0.07 ($\varphi = (\Delta T_p/T_p)/\Delta(\log \nu)$), which is typical for spin-glass behavior ($0.01 < \varphi < 0.08$).[56] The isothermal magnetization at 1.8 K shows no clear hysteresis loop (Figure S6b).

DOI: 10.1021/acs.inorgchem.5b00074
Inorg. Chem. 2015, 54, 2976−2982

The $\chi_M T$ value of **2** is 2.89 cm^3 mol^{-1} K at 300 K, higher than the expected value for one spin-only Co(II) ion due to the spin−orbit coupling (Figure 4a). By lowering the temperature, $\chi_M T$ values first decrease to 0.97 cm^3 mol^{-1} K at 11.96 K, which can be attributed to the antiferromagnetic interactions and/or spin−orbit coupling. $\chi_M T$ increases rapidly in the range 10 to 2.8 K, which might be attributed to the spin canting and was further evidenced by the field dependence of magnetization at 2 K.[57] The M vs H curve shows an abrupt increase to above 0.34 Nβ before 1400 Oe and further reaches linearly to 0.8 Nβ without saturation (Figure 4b). The second decrease of $\chi_M T$ would be attributed to the interchain antiferromagnetic interactions. Fitting the data with the Fisher 1D model in the range 75−300 K gives $J = -19.67$ cm^{-1} and $g = 2.62$ (Figure S5b). The negative J indicates antiferromagnetic interactions between Co(II) ions in the chain. The antiferromagnetic behavior of **2** can be understood on the basis of its structural feature: the exchange pathway between two adjacent Co(II) ions consists of one bidentate-bridged OH with the Co−O−Co angle of 117.26(3)°, which surpasses the range for ferromagnetic exchange pathways (90 ± 14°).[58] The ac magnetic susceptibility for **2** was measured. However, no frequency-dependent ac susceptibility was observed under zero dc field (Figure S7).

The room-temperature $\chi_M T$ value of **3** is 14.97 cm^3 mol^{-1} K (Figure 5a), which is larger than that expected for seven spin-only Co(II) ions (13.13 cm^3 K mol^{-1}). This phenomenon is very common for the Co(II) ion due to its strong spin−orbit coupling. When the temperature is lowered, $\chi_M T$ decreases rapidly to 4.35 cm^3 mol^{-1} K at 2 K, which results from the spin−orbit coupling and/or antiferromagnetic interactions. The field dependence of magnetization for **3** at 2 K displays an increase of the magnetization along with the increasing fields without saturation even at 70 kOe (Figure 5b). To further study the magnetization dynamics of **3**, ac susceptibility was measured at zero dc field. Interestingly, frequency-dependent χ_M'' signals were observed below 5 K, suggesting slow relaxation of the magnetization for **3**. However, peaks of χ_M'' were not observed above 2 K (Figure S8). Such phenomena may be caused by fast quantum tunneling of magnetization, which could be well suppressed by applying an external magnetic field. In this case, the field dependence of the relaxation time was measured. The optimized external field for the slowest relaxation time (τ) is 1800 Oe (Figure S9). Peaks were observed in χ'' at low temperatures when an external dc field (1800 Oe) was applied (Figure 5d). Cole−Cole plots can be well fitted by the modified Debye function (Figure 5e),[59] to give α values less than 0.45, indicative of a wide distribution of relaxation time.[60] The $\ln(\tau)-1/T$ plot shows a deviation from linearity, which could be explained as a transition from an Orbach process at high temperature to a non-Orbach process at low temperature, such as the direct process or a Raman process. The relaxation time from 2.6 to 7 K obeys the Arrhenius law and gives $\tau_0 = 2.20 \times 10^{-8}$ s and $\Delta_\tau/k_B = 34$ K (Figure 5f), which lies well for single-molecule magnets (SMMs).[61]

Nowadays, transition metal clusters can be successfully assembled into higher dimensional frameworks in constructing molecular magnetic materials. The reported 3D Co(II)-cluster-based MOFs showing SMM behavior are mostly based on trinuclear and tetranuclear cores.[62,63] To the best of our knowledge, **3** is the first example of MOFs showing SMM behavior based on magnetic Co_7 clusters. Such a combination of molecular magnetic clusters and large ligand in a multidimensional structure would enable low-dimensional magnetism without magnetic ordering because a large ligand can effectively separate the magnetic interaction between the clusters. This work illustrates an effective method of incorporating multinuclear cobalt clusters into a 3D framework showing SMM behavior.[64]

CONCLUSION

Three Co(II)-based complexes constructed from a bifunctional organic linker have been structurally and magnetically studied. Complexes **1** and **2** consist of similar 1D Co(II) chains bridged by different anions (Cl^- for **1** and OH^- for **2**), and this small discrepancy leads to their different magnetic properties (spin-glass for **1** and antiferromagnetic interaction for **2**). MOF **3** is a 3D 6-connected framework based on Co_7 clusters displaying interesting field-induced SMM behavior. The modification of magnetic behaviors by tuning metal nodes in MOFs provides new insights into the construction of new molecular materials with targeted magnetic properties.

ASSOCIATED CONTENT

Supporting Information

Additional structure figures (Figures S1, S2), PXRD (Figure S3), TGA (Figure S4), and CIF files for **1**−**3**. These materials are available free of charge via the Internet at http://pubs.acs.org.

AUTHOR INFORMATION

Corresponding Authors

*E-mail: naxu@nankai.edu.cn.
*E-mail: pcheng@nankai.edu.cn.

Author Contributions

†These authors contributed equally to this work.

Notes

The authors declare no competing financial interest.

ACKNOWLEDGMENTS

The financial support of the "973 Program" (2012CB821702), the NSFC (91422302 and 21171100), the MOE (IRT-13R30 and IRT13022), and the 111 Project (B12015) is acknowledged.

REFERENCES

(1) Suh, M. P.; Park, H. J.; Prasad, T. K.; Lim, D.-W. *Chem. Rev.* **2012**, *112*, 782−835.
(2) Li, J.-R.; Sculley, J.; Zhou, H.-C. *Chem. Rev.* **2012**, *112*, 869−932.
(3) Sumida, K.; Rogow, D. L.; Mason, J. A.; McDonald, T. M.; Bloch, E. D.; Herm, Z. R.; Bae, T.-H.; Long, J. R. *Chem. Rev.* **2012**, *112*, 724−781.
(4) Liu, D.; Lang, J.-P.; Abrahams, B. F. *J. Am. Chem. Soc.* **2011**, *133*, 11042−11045.
(5) Liu, D.; Ren, Z.-G.; Li, H.-X.; Lang, J.-P.; Li, N.-Y.; Abrahams, B. F. *Angew. Chem., Int. Ed.* **2010**, *49*, 4767−4770.
(6) Yoon, M.; Srirambalaji, R.; Kim, K. *Chem. Rev.* **2012**, *112*, 1196−1231.
(7) Cui, Y.; Yue, Y.; Qian, G.; Chen, B. *Chem. Rev.* **2012**, *112*, 1126−1162.
(8) Shustova, N. B.; Cozzolino, A. F.; Reineke, S.; Baldo, M.; Dincă, M. *J. Am. Chem. Soc.* **2013**, *135*, 13326−13329.
(9) Li, K.; Olson, D. H.; Lee, J. Y.; Bi, W.; Wu, K.; Yuen, T.; Xu, Q.; Li, J. *Adv. Funct. Mater.* **2008**, *18*, 2205−2214.
(10) Coronado, E.; Mínguez Espallargas, G. *Chem. Soc. Rev.* **2013**, *42*, 1525−1539.

DOI: 10.1021/acs.inorgchem.5b00074
Inorg. Chem. 2015, 54, 2976−2982

(11) Paz, F. A. A.; Klinowski, J.; Vilela, S. M. F.; Tomé, J. P. C.; Cavaleiro, J. A. S.; Rocha, J. *Chem. Soc. Rev.* **2012**, *41*, 1088−1110.
(12) *Metal-Organic Frameworks. Applications from Catalysis to Gas Storage*; Farrusseng, D., Ed.; Wiley−VCH Verlag & Co. KGaA: Weinheim, Germany, 2011.
(13) *Metal-Organic Frameworks. Design and Application*; MacGillivray, L., Ed.; Wiley−VCH Verlag & Co. KGaA: Weinheim, Germany, 2011.
(14) Li, J. R.; Timmons, D. J.; Zhou, H. C. *J. Am. Chem. Soc.* **2009**, *131*, 6368−6369.
(15) Zhou, Y. L.; Zeng, M. H.; Wei, L. Q.; Li, B. W.; Kurmoo, M. *Chem. Mater.* **2010**, *22*, 4295−4303.
(16) Leng, J. D.; Liu, J. L.; Tong, M. L. *Chem. Commun.* **2012**, *48*, 5286−5288.
(17) Escuer, A.; Vlahopoulou, G.; Mautner, F. A. *Inorg. Chem.* **2011**, *50*, 2717−2719.
(18) Schubert, U. *Chem. Soc. Rev.* **2011**, *40*, 575−582.
(19) Perry, J. J.; Perman, J. A.; Zaworotko, M. J. *Chem. Soc. Rev.* **2009**, *38*, 1400−1417.
(20) Stock, N.; Biswas, S. *Chem. Rev.* **2012**, *112*, 933−969.
(21) Li, Y.-M.; Lun, H.-J.; Xiao, C.-Y.; Xu, Y.-Q.; Wu, L.; Yang, J.-H.; Niu, J.-Y.; Xiang, S.-C. *Chem. Commun.* **2014**, *50*, 8558−8560.
(22) Chen, D.; Zhang, X.; Shi, W.; Cheng, P. *Cryst. Growth Des.* **2014**, *14*, 6261−6268.
(23) Ma, X.; Zhang, Z.; Shi, W.; Li, L.; Zou, J.; Cheng, P. *Chem. Commun.* **2014**, *50*, 6340−6342.
(24) Shi, P.; Chen, Z.; Xiong, G.; Shen, B.; Sun, J.-Z.; Cheng, P.; Zhao, B. *Cryst. Growth Des.* **2012**, *12*, 5203−5210.
(25) Li, H.-H.; Shi, W.; Xu, N.; Zhang, Z.-J.; Niu, Z.; Han, T.; Cheng, P. *Cryst. Growth Des.* **2012**, *12*, 2602−2612.
(26) Zhuang, W.; Sun, H.; Xu, H.; Wang, Z.; Gao, S.; Jin, L. *Chem. Commun.* **2010**, *46*, 4339−4341.
(27) Cheng, X.-N.; Zhang, W.-X.; Lin, Y.-Y.; Zheng, Y.-Z.; Chen, X.-M. *Adv. Mater.* **2007**, *19*, 1494.
(28) Liu, K.; Shi, W.; Cheng, P. *Dalton Trans.* **2011**, *40*, 8475−8490.
(29) Zhang, S.-Y.; Zhang, Z.-J.; Shi, W.; Zhao, B.; Cheng, P.; Liao, D.-Z.; Yan, S.-P. *Dalton Trans.* **2011**, *40*, 7993−8002.
(30) Zhang, S.-Y.; Shi, W.; Lan, Y.; Xu, N.; Zhao, X.-Q.; Powell, A. K.; Zhao, B.; Cheng, P.; Liao, D.-Z.; Yan, S.-P. *Chem. Commun.* **2011**, *47*, 2859−2861.
(31) Chen, Y.; Ma, J.-G.; Zhang, J.-J.; Shi, W.; Cheng, P.; Liao, D.-Z.; Yan, S.-P. *Chem. Commun.* **2010**, *46*, 5073−5075.
(32) Huang, F.-P.; Zhang, Q.; Yu, Q.; Bian, H.-D.; Liang, H.; Yan, S.-P.; Liao, D.-Z.; Cheng, P. *Cryst. Growth Des.* **2012**, *12*, 1890−1898.
(33) Huang, F.-P.; Tian, J.-L.; Gu, W.; Liu, X.; Yan, S.-P.; Liao, D.-Z.; Cheng, P. *Cryst. Growth Des.* **2010**, *10*, 1145−1154.
(34) Zhang, W.-H.; Song, Y.-L.; Ren, Z.-G.; Li, H.-X.; Li, L.-L.; Zhang, Y.; Lang, J.-P. *Inorg. Chem.* **2007**, *46*, 6647−6660.
(35) Zou, J.-Y.; Shi, W.; Xu, N.; Li, L.-L.; Tang, J.-K.; Gao, H.-L.; Cui, J.-Z.; Cheng, P. *Chem. Commun.* **2013**, *49*, 8226−8228.
(36) Chen, D.-M.; Shi, W.; Cheng, P. *Chem. Commun.* **2015**, *51*, 370−372.
(37) Gao, W.-Y.; Cai, R.; Meng, L.; Wojtas, L.; Zhou, W.; Yildirim, T.; Shi, X.; Ma, S. *Chem. Commun.* **2013**, *49*, 10516−10518.
(38) Naik, A.; Marchand-Brynaert, J.; Garcia, Y. *Synthesis* **2008**, 149−154.
(39) Sheldrick, G. M. *Acta Crystallogr.* **2008**, *A64*, 112−122.
(40) *PLATON* program: Spek, A. L. *Acta Crystallogr., Sect. A* **1990**, *46*, 194−201.
(41) Blatov, V. A. *IUCr Comput. Comm. Newsletter* **2006**, *7*, 4−38.
(42) D. Brown, I.; Altermatt, D. *Acta Crystallogr.* **1985**, *B41*, 244−247.
(43) Ferguson, A.; Parkin, A.; Sanchez-Benitez, J.; Kamenev, K.; Wernsdorfer, W.; Murrie, M. *Chem. Commun.* **2007**, *118*, 3473−3475.
(44) Chibotaru, L. F.; Ungur, L.; Aronica, C.; Elmoll, H.; Pilet, G.; Luneau, D. *J. Am. Chem. Soc.* **2008**, *130*, 12445−12455.
(45) Cheng, X.-N.; Zhang, W.-X.; Lin, Y.-Y.; Zheng, Y.-Z.; Chen, X.-M. *Adv. Mater.* **2007**, *19*, 1494−1498.
(46) Zhang, Y.-Z.; Wernsdorfer, W.; Pan, F.; Wang, Z.-M.; Gao, S. *Chem. Commun.* **2006**, 3302−3304.
(47) Yang, E.-C.; Liu, Z.-Y.; Wu, X.-Y.; Zhao, X.-J. *Chem. Commun.* **2011**, *47*, 8629−8631.
(48) Klöwer, F.; Lan, Y.; Nehrkorn, J.; Waldmann, O.; Anson, C. E.; Powell, A. K. *Chem.—Eur. J.* **2009**, *15*, 7413−7422.
(49) Mondal, K. C.; Kostakis, G. E.; Lan, Y.; Anson, C. E.; Powell, A. K. *Inorg. Chem.* **2009**, *48*, 9205−9213.
(50) Chandrasekhar, V.; Pandian, B. M.; Azhakar, R.; Vittal, J. J.; Clérac, R. *Inorg. Chem.* **2007**, *46*, 5140−5142.
(51) Ahmad, M.; Sharma, M. K.; Das, R.; Poddar, P.; Bharadwaj, P. K. *Cryst. Growth Des.* **2012**, *12*, 1571−1578.
(52) Yang, Q.; Zhao, J.-P.; Song, W.-C.; Bu, X.-H. *Dalton Trans.* **2012**, *41*, 6272−6276.
(53) Fisher, M. E. *Am. J. Phys.* **1964**, *32*, 343−345.
(54) Liu, T.-F.; Fu, D.; Gao, S.; Zhang, Y.-Z.; Sun, H.-L.; Su, G.; Liu, Y.-J. *J. Am. Chem. Soc.* **2003**, *125*, 13976−13977.
(55) Ouellette, W.; Prosvirin, A. V.; Whitenack, K.; Dunbar, K. R.; Zubieta, J. *Angew. Chem., Int. Ed.* **2009**, *48*, 2140−2143.
(56) Mydosh, J. A. *Spin Glasses: An Experimental Introduction*; Taylor & Francis: London, 1993.
(57) Zhao, J.-P.; Yang, Q.; Liu, Z.-Y.; Zhao, R.; Hu, B.-W.; Du, M.; Chang, Z.; Bu, X.-H. *Chem. Commun.* **2012**, *48*, 6568−6570.
(58) Kahn, O. *Molecular Magnetism*; VCH: Weiheim, 1993.
(59) Carlin, R. L. *Magnetochemistry*; Springer-Verlag: Berlin, 1986.
(60) Hagiwara, M. *J. Magn. Magn. Mater.* **1998**, 177−181.
(61) Hang, Y.-Z.; Gao, S.; Sato, O. *Dalton Trans.* **2014**, *47*, 8629−8631.
(62) Kurmoo, M. *Chem. Soc. Rev.* **2009**, *38*, 1353−1379.
(63) Wu, B. Y.; Yang, C. I.; Nakano, M.; Lee, G. H. *Dalton Trans.* **2014**, *43*, 47−50.
(64) Galloway, K. W.; Schmidtmann, M.; Sanchez-Benitez, J.; Kamenev, K. V.; Wernsdorfer, W.; Murrie, M. *Dalton Trans.* **2010**, *39*, 4727−4729.

DOI: 10.1021/acs.inorgchem.5b00074
Inorg. Chem. 2015, 54, 2976−2982